MULTIVARIABLE PID CONTROLLERS VIA LMI APPROACH APPLIED TO A GYROMETER

Boivin B. Rambault L. Coirault P. Mehdi D. Bosche J.

rambault(or boivin or coirault or mehdi)@esip.univ-poitiers.fr
LAII-ESIP 40 Avenue de Recteur Pineau 86022 Poitiers -FRANCE
Telephone number: (33) 549 453 642
Fax-number: (33) 549 454 034

Keywords: Industrial application, Multivariable PID, Stabilization, LMI.

Abstract

The aim of this paper is to develop the design of a sensor and improve its characteristics by using the control theory. The sensor studied is a gyrometer. The gyrometer is an angular velocity sensor used for the design of the instruments of navigation for aeronautics. Its principle is based on the detection of Coriolis accelerations introduced by the mechanical vibrations. This sensor brings into mechanical phenomena (vibrations of a resonator) and electromagnetic (excitation and detection of these vibrations). The objective of the controller applied to this system is to guarantee the stability of the sensor. The main objective is to respect the PID structure of real time implementation. To solve this problem, this paper proposes to use a methodology based on LMI.

1 Introduction

This paper presents the study of the mathematical model of a vibrating gyrometer and its control using a multivariable PID controller. The main interest of this paper is to purpose an effective method to design a PID controller for a MIMO industrial system. The gyrometer is an angular velocity sensor used for the design of the instruments of navigation for aeronautics. Its principle is based on the detection of Coriolis accelerations introduced by the mechanical vibrations. This sensor brings into mechanical phenomena (vibrations of a resonator) and electromagnetic (excitation and detection of these vibrations). The objective of the controller applied to this system is to guarantee the linearity of the sensor. The output signal must be represented as follow:

$i_s = K_1 \left(\Omega + K_0\right)$

with constants K_0 and K_1. K_1 represents the scale factor, K_0 the bias and Ω the real rotate speed to measure. The difficulty lies in the fact that, on the one hand, the various electric signals are oscillating and on the other hand, the control signals and the signals of measurements are multiplexed. They cannot coexist simultaneously. A continuous time controller has been tested by the company Thales Avionics. The choice of PID structure respects the industrial constraint in order to use the existing controller. To solve the problem of PID controller design it is purposed to design an equivalent static output feedback controller.

The second section presents the algorithm used to design the PID. The third section presents the physical principle of the gyrometer and its model used for the multivariable PID controller design. The fourth section concerns numerical results.

[0]This work is funded by Thales Avionics. The authors gratefully acknowledges the support of this research by Thales Avionics through provision of a research team

2 PID controller design

Proportional Integral Derivative controllers are still widely used in industrial process. Its popularity is due to its simplicity, it needs only three parameters to tune. However, the three PID parameters should be tune appropriately in order to satisfy control performance.

The problem of design a multivariable PID controller is formulated in a LMI framework (1).

Concerning the application proposed in this paper, the PID controller is designed with experimental approach. The objective is to achieve a better performance of the control than the initial controller.

The method used in this paper concerns the feedback stabilization. In this section, we just summarize the technic. For more details the reader is invited to see (4).

The first step is to transform the PID controller to static output feedback.

Consider the linear time invariant system:

$$\dot{x} = Ax + Bu, y = Cx \tag{1}$$

and the following PID controller

$$u = F_1 y + F_2 \int_0^t y dt + F_3 \frac{dy}{dt} \tag{2}$$

where $x(t) \in R^n$ represents the state vector, $u(t) \in R^l$ represents the control vector and $y(t) \in R^m$ represents the output vector.

F_1, F_2, F_3 are matrices to be designed.

Lets consider $z = [z_1^T z_2^T]$ the new state space vector where: $z_1 = x$ and $z_2 = \int_0^t y dt$.

$\dot{z} = \bar{A}z + \bar{B}u$

$\bar{y}_i = \bar{C}_i z \; i = 1, 2, 3$

where $\bar{A} = \begin{bmatrix} A & 0 \\ C & 0 \end{bmatrix}$ $\bar{B} = \begin{bmatrix} B \\ 0 \end{bmatrix}$ $\bar{C}_1 = [C \; 0]$ $\bar{C}_2 = [0 \; I]$ $\bar{C}_3 = [CA \; 0]$

The control law $u = F_1\bar{y}_1 + F_2\bar{y}_2 + F_3\bar{y}_3 + F_3CBu$.

Suppose the matrix $(I - F_3CB)$ is invertible.

$\bar{y} = [\bar{y}_1^T \bar{y}_2^T \bar{y}_3^T]^T$ $\bar{C} = [\bar{C}_1^T \bar{C}_2^T \bar{C}_3^T]^T$

$\bar{F} = [\bar{F}_1 \bar{F}_2 \bar{F}_3] = [(I - F_3CB)^{-1}F_1 \; (I - F_3CB)^{-1}F_2 \; (I - F_3CB)^{-1}F_3]$

So the problem of PID controller design reduces so that of static output feedback controller design apply of the following system.

$\dot{z} = \bar{A}z + \bar{B}u$ $\bar{y} = \bar{C}z$ $u = \bar{F}\bar{y}$

The objective of static output feedback problem is to find F such that $u = F.y$.

where the closed loop system $\dot{x} = (A + BFC)x$ is asymptotically stable.

Lemma 1 (2). *System (1) is stabilizable via static output feedback if and only if there exist matrices $P > 0$ and F satisfying the following matrix inequality:* $A^TP + PA - PBB^TP + (B^TP + FC)^T(B^TP + FC) < 0$

The solution is described by the following LMI algorithm described in the paper (4).

Initial data: System's state space realization $(\bar{A}, \bar{B}, \bar{C})$.

Step 1: Choose $Q_0 > 0$ and solve P for the Riccati equation: $\bar{A}^TP + P\bar{A} - P\bar{B}\bar{B}^TP + Q_0 = 0, P > 0$.

Set $i = 1$ and $X_1 = P$.

Step 2: Solve the following optimization problem for $P_i, \bar{F}$ and α_i: Minimize α_i subject to the constraint LMIs:

$$\begin{bmatrix} \Sigma_{1i} & (\bar{B}^TP_i + \bar{F}\bar{C})^T \\ \bar{B}^TP_i + \bar{F}\bar{C} & -I \end{bmatrix} < 0, P_i > 0$$

$$I + (\bar{C}\bar{B}\bar{F}_3)^T + \bar{C}\bar{B}\bar{F}_3 > 0$$

where $\Sigma_{1i} = \bar{A}^TP_i + P_i\bar{A} - X_i\bar{B}\bar{B}^TP_i - P_i\bar{B}\bar{B}^TX_i + X_i\bar{B}\bar{B}^TX_i - \alpha_iP_i$. Denote by α_i^* the minimized value of α_i.

Step 3: If $\alpha_i^* \leq 0$, the matrix pair $(P_i, \bar{F})$ solves static output feedback problem. Stop. Otherwise go to Step 4.

Step 4: Solve the optimization problem for P_i and $\bar{F}$: Minimize $tr(P_i)$ subject to the constraint following LMIs with $\alpha_i = \alpha_i^*$ (tr stands for the trace of a square matrix):

$$\begin{bmatrix} \Sigma_{1i} & (\bar{B}^TP_i + \bar{F}\bar{C})^T \\ \bar{B}^TP_i + \bar{F}\bar{C} & -I \end{bmatrix} < 0, P_i > 0$$

$$I + (\bar{C}\bar{B}\bar{F}_3)^T + \bar{C}\bar{B}\bar{F}_3 > 0$$

where $\Sigma_{1i} = \bar{A}^TP_i + P_i\bar{A} - X_i\bar{B}\bar{B}^TP_i - P_i\bar{B}\bar{B}^TX_i + X_i\bar{B}\bar{B}^TX_i - \alpha_iP_i$. Denote by P_i^* the optimal value of P_i.

Step 5: If $||X_i\bar{B} - P_i^*\bar{B}|| < \varepsilon$, where ε is a prescribes tolerance, go to Step 6; otherwise set $i = i + 1$, $X_i = P_i^*$, and go to Step 2.

Step 6: It cannot be decided by this algorithm whether static output feedback problem is solvable. Stop.

The properties of solution series α_i^* and P_i^* are given in (2).

This technique can be used to design multivariable PID with H_2 or H_∞ approach.

3 Modelling of gyrometer

3.1 physical description

There exits many technics to perform gyroscope. One of them is based on the Coriolis effect. The gyroscope consists of an elastic body such that one of its resonant modes is excited to constant amplitude vibrations (drive mode). Inducing rate about a particular body-fixed axis excites a different resonant mode into vibration (output mode). Generally, the rate by which the energy transfers from the first to the second mode is a measure of the induced rate. In an open-loop mode, the amplitude of the second mode is a measure to the rate, while in a closed-loop mode the rebalancing force is that measure. Electrostatic forces are the most commonly used actuation forces to excite the first mode vibrations. The second mode sensing is mostly done by capacitive or piezoresistive sensing. For this application, the vibrating gyroscope employs inductance sensing for the second mode vibrations.

Fig. 1 shows a schematic view of the gyroscope. It is composed of an elastic hollow cylinder, and a set of coils distributed around the cylinder. A permanent magnetic field is induced by a d.c. current exciting the polarization coils.

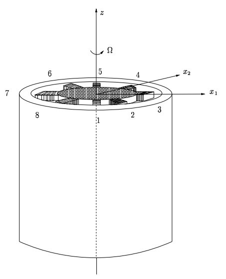

Fig. 1. Gyroscope structure: polarization coils (1 to 8) excitation coils (1,3,5,7), rebalancing coils (2,4,6,8)

By applying an alternating current to the excitation coils, a first mechanical mode of the elastic cylinder is excited into vibrations (fig. 2).

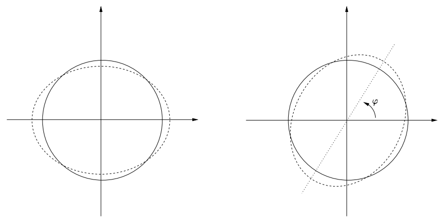

Fig. 2. Oscillatory motion of mass

The oscillation of the cylinder is an elliptical motion, that vibrates at the frequency of the magnetic field. If the cylinder is subjected to revolutions around z-axis with an angular rate $\Omega(t)$, the elliptical motion is driven with the cylinder, with an opposite and lower speed $\varphi(t) = -\frac{k_c}{2}\Omega(t)$, where k_c depends on the gyroscope geometry (see fig. 3).

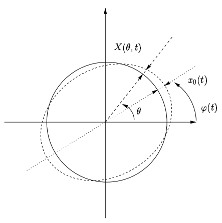

Fig. 3. elliptical motion during rotation

$X(\theta, t) = x_0(t)\cos(2(\theta - \varphi))$ is the displacement of the cylinder in the radial direction. Projecting $X(\theta, t)$ on the body-fixed axis x_1 and x_2 gives (see fig. 4)

$$X(\theta, t) = x_1(t)\cos(2\theta) + x_2(t)\sin(2\theta)$$

with

$$\begin{aligned} x_1(t) &= x_0(t)\cos(2\varphi(t)) \\ x_2(t) &= x_0(t)\sin(2\varphi(t)) \end{aligned}$$

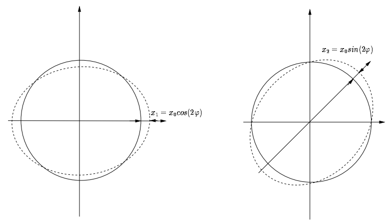

Fig. 4. Projection of the elliptical motion on the body-fixed axis

$x_1(t)$ and $x_2(t)$ represent the amplitudes of the resulting oscillatory motion in two fixed points belonging to the cylinder. They induce electromagnetic currents in coils. To maintain constant the elliptical motion (i.e. $\varphi(t) = 0$) needs to generate a second vibratory mode along x_1 and x_2 axes (fig. 5). In closed-loop mode, the electromagnetic counterbalancing forces F_1 and F_2 are such that $x_2(t) = 0$.

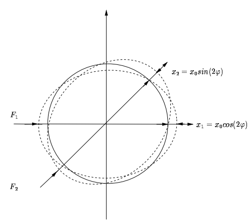

Fig. 5. Counterbalancing forces F_1 and F_2

3.2 Mathematical model used for the gyrometer

The state space representation is given by (3)

$$\left\{ \begin{aligned} \begin{bmatrix} \ddot{x}_1 \\ \dot{x}_1 \\ \ddot{x}_2 \\ \dot{x}_2 \end{bmatrix} &= \begin{bmatrix} -\frac{A}{M} & -\frac{K}{M} & \frac{2Mc\Omega}{M} & 0 \\ 1 & 0 & 0 & 0 \\ -\frac{2Mc\Omega}{M} & 0 & -\frac{A}{M} & -\frac{K}{M} \\ 0 & 0 & 1 & 0 \end{bmatrix} \begin{bmatrix} \dot{x}_1 \\ x_1 \\ \dot{x}_2 \\ x_2 \end{bmatrix} \\ &+ \begin{bmatrix} \frac{G_{exc}{K_z}^2}{M} & 0 \\ 0 & 0 \\ 0 & \frac{G_{exc}{K_z}^2}{M} \\ 0 & 0 \end{bmatrix} \begin{bmatrix} i_1 \\ i_2 \end{bmatrix} \\ \begin{bmatrix} u_1 \\ u_2 \end{bmatrix} &= \begin{bmatrix} G_{det} & 0 & 0 & 0 \\ 0 & 0 & G_{det} & 0 \end{bmatrix} \begin{bmatrix} \dot{x}_1 \\ x_1 \\ \dot{x}_2 \\ x_2 \end{bmatrix} \end{aligned} \right. \tag{3}$$

where

- M mass of cylinder,
- K coefficient for the stiffness,
- A Damping ratio,
- M_c mass of Coriolis,
- K_z coefficient that depends on longitudinal position of plan of excitation/detection,
- G_{exc} gain for the excitation,
- G_{det} gain for the detection.

The model defined above has two inputs and two outputs. Furthermore, it is nonlinear and from the rotate speed, a coupling between the axes 1 and 2 appeared.

$$U_1(p) = \frac{G_{det}G_{exc}K_z^2 p}{Mp^2 + Ap + K} I_1(p) + \frac{2M_c\Omega p}{Mp^2 + Ap + K} U_2(p)$$

and

$$U_2(p) = \frac{G_{det}G_{exc}K_z^2 p}{Mp^2 + Ap + K} I_2(p) - \frac{2M_c\Omega p}{Mp^2 + Ap + K} U_1(p)$$

The Bode plot for functions $H_i(p) = \dfrac{U_i(p)}{I_i(p)}$ is given on figure (6).

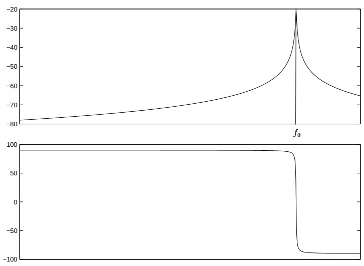

Fig. 6 Bode plot for a subsystem

f_0 represents the frequency of resonance for the considered system. The properties which are consided take place around this frequency. To highlight those properties and to be able to control the system around f_0, we purpose to shift the model in low frequency. To do this, we uses the complex signal with the help of Hilbert transform.

3.3 Low frequency mathematical model

The various signals in the system can be written as:

$$x = X\cos(\omega_0 t + \Phi) \tag{4}$$

It is possible to introduce the analytical signal described by (5).

$$x = \underline{X} e^{j\omega_0 t} \tag{5}$$

where $\underline{X} = Xe^{j\Phi}$ represents the complex envelope of the signal.

By simplifying by $e^{j\omega_0}$ and separating the imaginary part and the real part, we obtain the state space following representation.

$$\begin{cases} \dot{X} &= AX + BI \\ U &= CX \end{cases}$$

with

$$X = \begin{bmatrix} \dot{X}_{1Re} & X_{1Re} & \dot{X}_{1Im} & X_{1Im} & \dot{X}_{2Re} & X_{2Re} & \dot{X}_{2Im} & X_{2Im} \end{bmatrix}^T$$

$$I = \begin{bmatrix} I_{1Re} & I_{1Im} & I_{2Re} & I_{2Im} \end{bmatrix}^T$$

$$U = \begin{bmatrix} U_{1Re} & U_{1Im} & U_{2Re} & U_{2Im} \end{bmatrix}^T$$

$$A = \left[\begin{array}{ccccc} -\frac{A}{M} & {w_0}^2 - \frac{K}{M} & 2w_0 & \frac{w_0 A}{M} & .. \\ 1 & 0 & 0 & 0 & .. \\ -2w_0 & -\frac{w_0 A}{M} & -\frac{A}{M} & {w_0}^2 - \frac{K}{M} & .. \\ 0 & 0 & 1 & 0 & .. \\ -\frac{2Mc\Omega}{M} & 0 & 0 & \frac{2w_0 M_c\Omega}{M} & .. \\ 0 & 0 & 0 & 0 & .. \\ 0 & -\frac{2w_0 M_c\Omega}{M} & -\frac{2Mc\Omega}{M} & 0 & .. \\ 0 & 0 & 0 & 0 & .. \end{array}\right.$$

$$\left.\begin{array}{cccc} \frac{2Mc\Omega}{M} & 0 & 0 & -\frac{2w_0 M_c\Omega}{M} \\ 0 & 0 & 0 & 0 \\ 0 & \frac{2w_0 M_c\Omega}{M} & \frac{2Mc\Omega}{M} & 0 \\ 0 & 0 & 0 & 0 \\ -\frac{A}{M} & {w_0}^2 - \frac{K}{M} & 2w_0 & \frac{w_0 A}{M} \\ 1 & 0 & 0 & 0 \\ -2w_0 & -\frac{w_0 A}{M} & -\frac{A}{M} & {w_0}^2 - \frac{K}{M} \\ 0 & 0 & 1 & 0 \end{array}\right]$$

$$B = \begin{bmatrix} \frac{G_{exc}{K_z}^2}{M} & 0 & 0 & 0 \\ 0 & 0 & 0 & 0 \\ 0 & \frac{G_{exc}{K_z}^2}{M} & 0 & 0 \\ 0 & 0 & 0 & 0 \\ 0 & 0 & \frac{G_{exc}{K_z}^2}{M} & 0 \\ 0 & 0 & 0 & 0 \\ 0 & 0 & 0 & \frac{G_{exc}{K_z}^2}{M} \\ 0 & 0 & 0 & 0 \end{bmatrix}$$

$$C = \begin{bmatrix} G_{det} & 0 & 0 & 0 \\ 0 & w_0 G_{det} & 0 & 0 \\ 0 & G_{det} & 0 & 0 \\ -w_0 G_{det} & 0 & 0 & 0 \\ 0 & 0 & G_{det} & 0 \\ 0 & 0 & 0 & w_0 G_{det} \\ 0 & 0 & 0 & G_{det} \\ 0 & 0 & -w_0 G_{det} & 0 \end{bmatrix}^T$$

4 Experimental results

In this section, we present the experiment results obtained by using the algorithm described in the previous section. We apply a step of speed to the gyrometer and stabilize the system by injection of currents in two directions. The current injection is controlled by the controller designed with the help of the method presented in this paper. The step of speed for this sensor is considered as perturbation. We solve the problem with the help of LMI Control Toolbox (Matlab) (3).

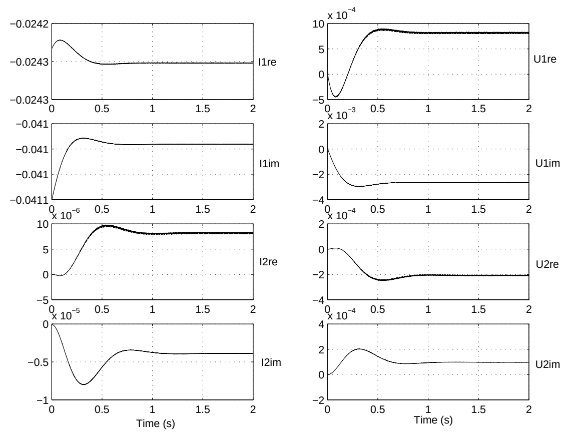

Fig. 7 Experimental results

The simplicity of the controller is interesting for real time implementation. The application proposed above concerns an industrial experiment. The main objective is to conserve the structure of real time implementation and to improve the controller performance.

5 Conclusion

This paper develops the control theory contribution to design a sensor applied to the aeronautic system. The two main problems are the multiplexing to avoid the magnetic coupling and the high quality factor of the cylinder. To overcome these problems, we propose to establish the model of the system in low frequency by the use of a Hilbert transform. An algorithm based on LMI technique have been proposed to solve a multivariable PID controller design in an industrial context. The main problem is to propose a methodology in order to keep the same real time structure. The results obtain by using this method are implemented with success in FPGA component.

The perspectives of this work concern the anlysis of robustness of the stability from two point of view. The first one is the experimental analysis of robustness and the second point of view is the mathematical analysis.

References

[1] S. Boyd, L. El Ghaoui, E. Feron, and V. Balakrishnan. *Linear Matrix Inequalities in System and and Control Theory*. SIAM, Philadelphia, 1994.

[2] Y.Y. Cao, J. Lam, and Y.X. Sun. Static output feedback stabilization: An ilmi approach. *Automatica*, 34:1641–1645, 1998.

[3] P. Gahinet, A. Nemirovski, J. Laub, and M. Chilali. *LMI Control Toolbox*. The Math Works Inc, 1995.

[4] F. Zheng, Q.G. Wang, and T.H. Lee. On the design of multivariable pid controllers via lmi approach. *Automatica*, 38:517–526, 2002.